



THE UNIVERSITY *of* EDINBURGH

Edinburgh Research Explorer

Refuting the hypothesis that semaphorin-3f/neuropilin-2 exclude blood vessels from the cap mesenchyme in the developing kidney

Citation for published version:

Munro, D, Hohenstein, P, Coate, TM & Davies, J 2017, 'Refuting the hypothesis that semaphorin-3f/neuropilin-2 exclude blood vessels from the cap mesenchyme in the developing kidney' *Developmental Dynamics*, vol. 246, no. 12, pp. 1047-1056. DOI: 10.1002/dvdy.24592

Digital Object Identifier (DOI):

[10.1002/dvdy.24592](https://doi.org/10.1002/dvdy.24592)

Link:

[Link to publication record in Edinburgh Research Explorer](#)

Document Version:

Peer reviewed version

Published In:

Developmental Dynamics

General rights

Copyright for the publications made accessible via the Edinburgh Research Explorer is retained by the author(s) and / or other copyright owners and it is a condition of accessing these publications that users recognise and abide by the legal requirements associated with these rights.


Take down policy

The University of Edinburgh has made every reasonable effort to ensure that Edinburgh Research Explorer content complies with UK legislation. If you believe that the public display of this file breaches copyright please contact openaccess@ed.ac.uk providing details, and we will remove access to the work immediately and investigate your claim.



Refuting the hypothesis that semaphorin-3f/neuropilin-2 exclude blood vessels from the cap mesenchyme in the developing kidney

Running title: *Sema3f* and *Nrp2* in kidney development

Authors: David A. D. Munro^{1*} , Peter Hohenstein², Thomas M. Coate³, and Jamie A. Davies¹

¹ Centre for Integrative Physiology, the University of Edinburgh, Hugh Robson Building, 15 George Square, Edinburgh, EH8 9XD, United Kingdom

² The Roslin Institute, the University of Edinburgh, Easter Bush, Edinburgh, EH25 9RG, United Kingdom

³ Georgetown University, Department of Biology, Regents Hall, Washington, DC 20007, United States

***Corresponding author:** David A. D. Munro¹ (E-mail: s1471287@sms.ed.ac.uk; Telephone: +44 131 650 3102)

Key words: metanephros; renal; anti-angiogenic; endothelial; vasculature; lymphatic

Key findings:

- Using gene expression data from the GUDMAP database, we selected *Sema3f* as an anti-angiogenic candidate gene that may exclude developing blood vessels from the cap mesenchyme (groups of nephron progenitor cells) in the murine metanephric (permanent) kidney.
- In the developing kidney, *Sema3f* is expressed in the cap mesenchyme, and its receptor, *Nrp2*, is expressed in endothelia that pattern in cycles around the caps in the nephrogenic zone.
- Genetic ablation of *Sema3f* and of *Nrp2* in mice demonstrated that they are not required for vascular exclusion from the cap mesenchyme.

Grant sponsor: Medical Research Council, Biotechnology and Biological Sciences Research Council, and National Institutes of Health. **Grant numbers:** MR/K501293/1, MR/K010735/1, BB/P013732/1, and NIH DC13107.

Accepted Articles are accepted, unedited articles for future issues, temporarily published online in advance of the final edited version.

© 2017 Wiley Periodicals, Inc.

Received: Jun 12, 2017; Revised: Aug 16, 2017; Accepted: Sep 16, 2017

Abstract

Background: During murine kidney development, new cortical blood vessels form and pattern in cycles that coincide with cycles of collecting duct branching and the accompanying splitting of the cap mesenchyme (nephron progenitor cell populations that 'cap' collecting duct ends). At no point in the patterning cycle do blood vessels enter the cap mesenchyme. We hypothesised that the exclusion of blood vessels from the cap mesenchyme may be controlled, at least in part, by an anti-angiogenic signal expressed by the cap mesenchyme cells.

Results: We show that semaphorin-3f (Sema3f), a known anti-angiogenic factor, is expressed in cap mesenchymal cells and its receptor, neuropilin-2 (Nrp2), is expressed by newly forming blood vessels in the cortex of the developing kidney. We hypothesised that Sema3f/Nrp2 signalling excludes vessels from the cap mesenchyme. Genetic ablation of *Sema3f* and of *Nrp2*, however, failed to result in vessels invading the cap mesenchyme.

Conclusions: Despite their complementary expression patterns, our data suggest that Sema3f and Nrp2 are dispensable for the exclusion of vessels from the cap mesenchyme during kidney development. These results should provoke additional experiments to ascertain the biological significance of Sema3f/Nrp2 expression in the developing kidney.

Introduction

In his *Collected Essays*, T.H. Huxley referred to '*The great tragedy of Science – the slaying of a beautiful hypothesis by an ugly fact*'. This report describes just such a slaying, of a hypothesis about how the arrangement of blood vessels is controlled in the developing kidney.

The major function of the adult kidney is to filter blood. Blood enters the kidneys via the renal arteries before being transported to the glomerular capillaries where small molecules are filtered into the Bowman's capsule. After filtration, useful molecules are reabsorbed by tubular cells and collected by peritubular capillaries, while waste and toxins are excreted as urine. This task requires a complex vasculature that must be assembled accurately during development.

Mouse metanephric (permanent) kidney development begins at E10.5 when the ureteric bud, the precursor of the collecting duct and ureter, evaginates from the caudal end of the Wolffian/nephric duct in response to glial cell-line-derived neurotrophic factor (GDNF; Sainio et al., 1997; Costantini & Kopan, 2010). The ureteric bud invades a mass of undifferentiated cells, the metanephrogenic mesenchyme, and begins to branch. As the ureteric bud branches, it induces nephron formation by provoking groups of nephron progenitor cells to undergo mesenchymal-to-epithelial transitions (Carroll et al., 2005). The nephron progenitor cells reciprocate by inducing branching of the ureteric bud (Majumdar et al., 2003; Costantini & Shakya, 2006; Cebrian et al., 2014). Prior to their differentiation, nephron progenitor cells situate around ureteric bud tips in cell populations known as the cap mesenchyme (they 'cap' the ureteric tips: Reinhoff, 1922). As the ureteric bud bifurcates, the overlaying cap mesenchymal population splits so that each new ureteric tip inherits a population of cap mesenchymal cells; this occurs in cycles throughout kidney development (Short et al., 2014).

Recently, we have shown that blood vessels pattern in cycles alongside the splitting of the cap mesenchyme and the branching of the ureteric bud in the developing kidney (Munro et

al., 2017). Vascular plexuses form around the cap mesenchyme, but they do not enter it. As the cap splits, endothelia migrate through the fissure to form new vascular plexuses. The mechanism by which this happens is not understood, but we hypothesised that at least part of the pattern, the avoidance of the cap mesenchyme by the vasculature, may arise through the cap mesenchyme expressing anti-angiogenic signalling molecules.

Certain class-3 semaphorins have a known capacity to act as anti-angiogenic signalling molecules. An example is semaphorin-3f (Sema3f; Bielenberg et al., 2004; Guttman-Raviv et al., 2007; Parker et al., 2010; Buehler et al., 2013; Guo et al., 2013). Although classically thought of as an axonal guidance molecule, Sema3f is highly expressed in multiple non-neuronal organs during development, such as the skin, lung, and kidney (Giger et al., 1998). Its functions in these tissue types are poorly understood.

In vascular development, Sema3f inhibits angiogenesis by interacting with its receptors on the endothelial cell membrane, neuropilin-1 (Nrp1; its low-affinity receptor) and neuropilin-2 (Nrp2; its high-affinity receptor; Guo et al., 2013; Sakurai et al., 2012). Sema3f/Nrp signalling results in the suppression of endothelial cell survival, proliferation, and migration (Guttman-Raviv et al., 2007; Procaccia et al., 2014; Nakayama et al., 2015).

Here, we characterise the expression patterns of Sema3f, Nrp1, and Nrp2 in the developing kidney. We show that they are expressed in a manner perfectly compatible with the hypothesis that they mediate exclusion of vasculature from caps, but go on to show that they are not, in fact, required for this aspect of vascular plexus patterning.

Results and Discussion

Selection of a cap mesenchyme-expressed, anti-angiogenic candidate gene

We previously demonstrated that renal endothelia pattern around, but do not enter, the cap mesenchyme in the nephrogenic zone of the developing kidney (Munro et al., 2017; Fig. 1A). Patterning occurs in cycles throughout most of embryonic kidney development, and we hypothesised that anti-angiogenic signals produced by the cap mesenchyme might be responsible for it being avascular. To test this, we generated a list of criteria to be met by cap mesenchyme-expressed candidate genes whose proteins might inhibit angiogenesis (Fig. 1B). We reviewed the literature to produce a list of 39 known anti-angiogenic genes and used microarray data from the GenitoUrinary Development Molecular Anatomy Project (GUDMAP) database (Brunskill et al., 2009; Harding et al., 2011) to assess their relative expression in the cap mesenchyme (Fig. 2). Of the genes investigated, *isthmin-1* (*Ism1*), *semaphorin-3f* (*Sema3f*), and *suppressor of cytokine signalling-3* (*Socs3*) met our initial criteria as candidate genes as they are highly expressed in the cap mesenchyme during the embryonic (E15.5) and early postnatal phase (at least at one age between P0-P4; Fig. 1C and Fig. 2).

The next condition to be met was that the relative expression of the gene had to be lower in the nephrogenic interstitium (which becomes vascularized) than the cap mesenchyme (which does not): this was true for all three of these candidate genes at E15.5 (Fig. 1D). The anti-angiogenic function of the protein also had to be mediated through cell non-autonomous signalling (i.e. via secretion from the cap mesenchyme or presentation on cap mesenchyme membranes so it can exert its effect on the nearby endothelia). *Socs3* is a Stat-inhibiting, intracellular protein (Starr et al., 1997) and its anti-angiogenic effect is endothelial-cell autonomous (Stahl et al., 2012; Rao et al., 2015): it was therefore discounted as a possible candidate gene.

Ism1 and Sema3f are secreted proteins, and their anti-angiogenic properties are exerted when they bind to their receptors on the endothelial cell membrane: receptor-ligand binding leads to the activation of signalling pathways that prevent endothelial cell survival and proliferation (Guttmann-Raviv et al., 2007; Xiang et al., 2011; Rao et al., 2015). Consequently, the receptors for Ism1 and Sema3f would need to be expressed in the plexus endothelia for them to transduce their signals. The receptors for Ism1 are integrin alpha-V (Itgav; Zhang et al., 2011) and 78 kDa glucose-regulated protein homolog (Grp78; Chen et al., 2014), and, based on microarray data, they were expressed weakly in renal endothelia (Fig. 1E). In contrast, the expression of the Sema3f receptors, neuropilin-1 and neuropilin-2 (Nrp1 and Nrp2, respectively), was high in renal endothelia (Fig. 1E). Based on these data, we further investigated the Sema3f/Nrp signalling pathway in vascular patterning in the nephrogenic zone.

Complementary expression pattern of Sema3f and Nrp2 in the developing kidney

The GUDMAP microarray data indicating that *Sema3f* is highly expressed in the cap mesenchyme at E15.5 has been validated at the RNA level by in situ hybridisation of whole-mount kidneys (data made available on GUDMAP by the McMahon lab; Fig 3A-A'). Although GUDMAP has little data on renal *Sema3f* expression prior to E15.5, data from the Allen Brain Atlas (Lein et al., 2007) show that *Sema3f* is also expressed in the kidney at E11.5 and E13.5 (Fig 3B-C'). At the earliest stages of renal organogenesis (E10.5-E11.5), the kidney is predominantly avascular, despite being surrounded by blood vessels (Munro et al., 2017). As *Sema3f* is expressed throughout the metanephrogenic mesenchyme at E11.5 (Fig. 3B-B'), its anti-angiogenic function could prevent premature renal vascularisation.

To investigate the localisation of the Sema3f protein, we stained whole-mount kidneys at E12.5 and E15.5 with anti-Sema3f. Kidneys were cleared with benzyl alcohol/benzyl benzoate (BABB) prior to imaging. At E12.5, Sema3f localises in tubular epithelia (in

agreement with Villegas and Tufro, 2002) and in the presumptive cap mesenchyme (Fig. 3D). At E15.5, we assessed co-localisation of *Sema3f* with the cap mesenchyme marker, integrin alpha-8 (Müller et al., 1997). *Sema3f* staining was not exclusive to the cap mesenchyme: it was observed in tubular epithelia, the cap mesenchyme, and the nephrogenic interstitium (Fig 3E). This is unsurprising as *Sema3f* is a secreted protein whose localisation is not restricted to the cell that produces it. Indeed, *Sema3f* would be required to exit the cap to bind to, and inhibit, endothelia in the nephrogenic interstitium.

To respond to *Sema3f*, the endothelia in the nephrogenic interstitium would have to express either *Nrp1*, *Nrp2*, or both. Confocal z-stack images of an E15.5 *Nrp2*-EGFP transgenic mouse kidney, made available on GUDMAP by Steven Potter's lab, indicated that *Nrp2* is expressed in proximal tubules and by an unknown cell type within the nephrogenic interstitium (Supplementary movie 1; adapted with permission from the Potter Lab). We examined whether the *Nrp2*⁺ cells within the nephrogenic interstitium were endothelial by co-staining with anti-*Nrp2* and anti-CD31 (an endothelial marker). The *Nrp2*⁺ cells were endothelial and were always present across the bifurcation site of the ureteric bud (42/42, 100%, CI^{95%} ± 1.19%; *n* = 42 bifurcation sites analysed in 1 kidney; Fig. 4A-C). Because new vascular plexuses form when endothelial cells migrate away from the bifurcation site (Munro et al., 2017; Fig. 4D), these *Nrp2*⁺ endothelia were situated in the precise location we would anticipate for them to be responding to *Sema3f*.

Expression of *Nrp1* and *Nrp2* in the developing kidney and ureter

Studies suggest that *Nrp1* and *Nrp2* are differentially expressed in arterial, venous, and lymphatic endothelia (Herzog et al., 2001). *Nrp2* is preferentially expressed in lymphatic vessels and veins, whereas *Nrp1* is expressed in arteries. We corroborated these findings by co-staining *Nrp1*⁺ and *Nrp2*⁺ endothelia with venous and lymphatic markers in the ureter (Fig. 5A-C'). The *Nrp2*⁺ endothelia in the ureter are lymphatic and venous (based on morphology [Fig. 5A] and as shown by co-staining with anti-Lyve-1 [Fig. 5B] and anti-EphB4 [Fig. 5C],

markers for lymph and vein respectively). The Nrp1⁺ endothelia in the ureter are arterial (as shown by lack of co-staining with anti-Nrp2 and anti-EphB4; Fig. 5C').

In the E11.5 and E12.5 kidney, almost all renal blood vessels expressed Nrp2, but few vessels expressed Nrp1 (Fig. 6A, B). By E13.5, Nrp1 had become highly expressed in renal arteries (Fig. 6C-E). The endothelial plexuses in the E13.5 kidney had many Nrp2⁺ cells, but few discernible Nrp1⁺ cells. In contrast, by E18.5 the plexus endothelia expressed Nrp2 as well as Nrp1 (Fig 6E, F). Nrp2 is highly enriched in endothelial tip cells (Siemerink et al., 2012). Based on the location of the Nrp2⁺ plexus endothelia at the vascular front (the site of new blood vessel formation), we speculate that these Nrp2⁺ cells are the endothelial tip cells in the kidney; however, there are no known specific endothelial tip cell markers to verify this hypothesis.

In the ureter, anti-Nrp2 staining is very strong in lymphatic vessels (Fig 5A-C). We next explored whether Nrp2⁺ lymphatic vessels form within the kidney. To do this, we cleared whole-mount E15.5 kidneys with BABB prior to imaging. We demonstrate that Nrp2⁺ lymphatic vessels form rings around the ureter and that these vessels connect with the lymphatic vessels in the renal pelvis (Fig 7A-B). In agreement with previous studies (Tanabe et al., 2012), renal Nrp2⁺ lymphatic vessels extend along the segmental vasculature from the renal pelvis (Fig 7C). The Nrp2⁺ lymphatic vessels in the kidney and ureter are in connection with a network of Nrp2⁺ lymphatic vessels that supply the adrenal gland, gonad, mesonephros, and ureter (Fig 7A; Supplementary movie 2).

Sema3f and Nrp2 are not required for exclusion of endothelia from the cap mesenchyme

After confirming the complementary expression pattern of Sema3f and Nrp2 in the nephrogenic zone, we tested the hypothesis that their interaction repels endothelia from the caps. Genetic ablation of *Sema3f* did not result in vessels entering the cap mesenchyme, as shown by co-staining for anti-Six2 (cap mesenchyme marker), anti-collagen IV (blood vessel

and ureteric bud basement membrane marker), and anti-CD31 (endothelial marker; Fig. 8A, C). Endothelial patterning was also normal in *Nrp2* null mouse kidneys (Fig. 8B, D), providing validation that signalling through the *Sema3f/Nrp2* pathway is not required for normal vascular plexus patterning around the cap mesenchyme.

In conclusion, we have demonstrated that, although *Sema3f* and its receptors (*Nrp1/2*) are expressed in a manner compatible with the hypothesis that their interaction excludes endothelia from the cap mesenchyme, signalling through the *Sema3f/Nrp* pathway is not required for vasculature repulsion from the cap. This lack of requirement for *Sema3f* and *Nrp2* could be the result of redundancy with another pathway, the result of compensatory expression of other genes (such as other class-3 semaphorins) in response to their loss, or simply that they are not involved in this aspect of vascular patterning.

We investigated the consequences of *Sema3f* and *Nrp2* deletion on vascular plexus patterning around the cap mesenchyme; however, *Sema3f* is also expressed by tubular cells in the kidney (Villegas and Tufro, 2002), and we have not eliminated the possibility that tubular expression of *Sema3f* could guide blood vessel patterning around nephrons/collecting ducts. Future studies should aim to reveal the significance of *Sema3f* and *Nrp2* expression in the development of the kidney.

Experimental procedures

Databases

Cap mesenchyme-expression of anti-angiogenic genes was examined using GUDMAP's gene expression search tool (http://www.gudmap.org/gudmap/pages/database_homepage.html). The microarray heatmap data for each gene was taken from the 'Developing Kidney (MOE430)' and 'Developing Kidney (ST1)' data sets (data retrieved May, 2017). The normalised heatmap data (red indicating high expression, blue indicating low expression, and black indicating expression that is close to the median) represents the binary logarithm of the average expression value of a given gene across an entire data set. For each probe set, experiments were performed in triplicate. Where there were two probe sets available for the expression of a given gene, the probe set with the most consistent data between replicate samples were shown. Where there were more than two probe sets available for the expression of a given gene, the probe set with the median values and/or colour were chosen for the analysis. The in situ hybridisation images showing *Sema3f* expression in the E15.5 kidney was submitted by the McMahon group (data retrieved from GUDMAP in May, 2017) and can be found at <http://www.gudmap.org/gudmap/pages/gene.html?genelid=MGI%3A1096347>. The confocal z-stack movie of the *Nrp2*-EGFP kidney was produced by the Potter group and can be found at http://www.gudmap.org/Resources/MouseStrains/Mouse_Strains_Summary.html under the heading 'Mouse strains generated by external sources' (data retrieved from GUDMAP in May, 2017). The in situ hybridisation images from the Allen Brain Atlas showing *Sema3f* expression at E11.5 can be found at <http://developingmouse.brain-map.org/experiment/show/100093437> (section 12/20; accessed May, 2017), and for E13.5 can be found at <http://developingmouse.brain-map.org/experiment/show/100076578> (section 7/16; accessed May, 2017). Using the above Allen Brain Atlas links, renal *Sema3f* expression can be observed in sections 11-13 and 16-17 of the E11.5 mouse (out of 20 sections), and in sections 6-10 and 15-16 of the E13.5 mouse (out of 16 sections).

Mice

Wild-type embryonic tissues were obtained from CD-1 mice that were killed by qualified staff of a UK Home Office-licensed animal house following the guidelines set under Schedule 1 of the UK Animals (Scientific Procedures) Act 1986. Experiments were approved and performed in accordance with the institutional guidelines and regulations as set by the University of Edinburgh. Tissue from P0 *Sema3f* knockout embryos was obtained from Georgetown University facilities according to locally approved procedures. The *Sema3f* mutant line was maintained in accordance with the NIH Animal Care and Use Committee. The caudal portions of euthanized P0 *Sema3f* mice were sent at 4°C to the University of Edinburgh where the kidneys were dissected and immunostained (for details, see Davies, 2006). The *Sema3f* knockout mouse line has previously been described (Walz et al., 2007). *Sema3f* mutant mice were bred for over 9 generations into a C57BL/6 genetic background (Charles River Laboratories, Frederick, MD). Tissue from E18.5 *Nrp2* transgenic mouse embryos was kindly provided by Alex Kolodkin and Qiang Wang (Johns Hopkins University). *Nrp2* mutant mice were bred into the C57BL/6 genetic background, and this mouse line has previously been described (Giger et al., 2000).

Immunohistochemistry

Embryonic kidneys were dissected as previously described (Davies, 2010). Kidneys were then fixed in methanol (pre-cooled at -20°C) for 1 hr. Fixed kidneys were either stored in methanol at -20°C (for up to 6 months) or directly processed following fixation. PBS was used to rinse off the methanol from the kidneys (3 x 20 mins) and the kidneys were blocked with 1x PBS with 5% donkey serum (Sigma, D9663) and 2.5% BSA (Sigma, A9647) for 1 hr-overnight. Kidneys were incubated with the following primary antibodies overnight at 4°C: rat-anti-CD31 (1:100; BD Pharmingen; 550274), goat-anti-collagen IV (1:100; Merckmillipore; AB769), rat-anti-EphB4 (1:100; abcam; ab73259), rabbit-anti-laminin (1:100; Sigma; L9393), rabbit-anti-Lyve1 (1:100; Abcam; ab33682), rabbit-anti-Nrp1 (1:100; abcam;

ab81321), goat-anti-Nrp2 (1:100; R&D systems; AF567), mouse-anti-pan cytokeratin (1:100; Sigma; C2562), rabbit-anti-Sema3f (1:100; abcam; ab39956), rabbit-anti-Six2 (1:250; Proteintech; 11562-1-AP), goat-anti-mouse-integrin alpha 8 (1:100; R&D systems; AF4076). Kidneys were then rinsed in 1x PBS (3 x 5 mins, then 3 x 1 hr) and subsequently incubated in Alexa Fluor conjugated secondary antibodies overnight at 4°C (emission λ of 350, 488, 594, 647; dilution of 1:200; Thermo Fisher Scientific). Finally, kidneys were washed in 1x PBS (3 x 5 mins, then 4 x 1 hr), before being mounted onto glass slides using Vectashield (Vectorlabs, H1000) as a mounting medium. Benzyl alcohol/benzyl benzoate (BABB) clearing whole-mount immunofluorescence was performed as previously described (Munro et al., 2017). BABB clearing was used for Fig. 3D-E and Fig. 7.

Microscopy

Images were captured using the Nikon A1R and Zeiss LSM800 confocal microscopes. Objective lenses of 4-60x were used (lenses were oil-immersed from 40x upwards).

Statistics and data presentation

95% confidence intervals for binary (yes/no) data were calculated using the formula $t=1.64\text{SQRT}(pq/n)+1/2n$, where t is the 95% confidence interval, p is the proportion positive, q is $1-p$, and n is the number examined. IMARIS (version 8.3.1) and Adobe premiere pro CC (2015) were used to prepare the supplementary movies.

Acknowledgements

We are extremely grateful to Prof. Alex Kolodkin and Dr Qiang Wang for supplying us with tissue from *Nrp2* knockout mouse embryos and for providing us with genotyping information. We are thankful to Dr Jane Armstrong, Prof Karen Chapman, Dr Melanie Lawrence, and Mr Christopher Mills for useful comments and advice. We would also like to express our gratitude to Dr Anisha Kubasik-Thayil of the IMPACT imaging facility at the University of Edinburgh for assistance with microscopy.

Author contributions

D.A.D.M designed and performed the experiments, analysed and collated the data, prepared the figures, and wrote the paper. P.H supervised the project and reviewed/edited the manuscript. T.M.C performed the experiments and reviewed/edited the manuscript. J.A.D supervised the project, designed the experiments, and reviewed/edited the manuscript.

Conflict of interest disclosure: None to declare.

References

- Bielenberg DR, Hida Y, Shimizu A, Kaipainen A, Kreuter M, Kim CC, Klagsbrun M. 2004. Semaphorin 3F, a chemorepellent for endothelial cells, induces a poorly vascularized, encapsulated, nonmetastatic tumor phenotype. *J Clin Invest.* **114**: 1260-71.
- Brunskill EW, Aronow BJ, Georgas K, Rumballe B, Valerius MT, Aronow J, Kaimal V, Jegga AG, Yu J, Grimmond S, McMahon AP, Patterson LT, Little MH, Potter SS. 2008. Atlas of gene expression in the developing kidney at microanatomic resolution. *Dev Cell.* **15**: 781-91.
- Buehler A, Sitaras N, Favret S, Bucher F, Berger S, Pielen A, Joyal JS, Juan AM, Martin G, Schlunck G, Agostini HT, Klagsbrun M, Smith LE, Sapienza P, Stahl A. 2013. Semaphorin 3F forms an anti-angiogenic barrier in outer retina. *FEBS Lett.* **587**: 1650-5.
- Carroll TJ, Park JS, Hayashi S, Majumdar A, McMahon AP. 2005. Wnt9b plays a central role in the regulation of mesenchymal to epithelial transitions underlying organogenesis of the mammalian urogenital system. *Dev Cell.* **9**: 283-92.
- Cebrian C, Asai N, D'Agati V, Costantini F. 2014. The number of fetal nephron progenitor cells limits ureteric branching and adult nephron endowment. *Cell Rep.* **7**: 127-37.
- Chen M, Zhang Y, Yu VC, Chong YS, Yoshioka T, Ge R. 2014. Isthmin targets cell-surface GRP78 and triggers apoptosis via induction of mitochondrial dysfunction. *Cell Death Differ.* **21**: 797-810.
- Costantini F, Kopan R. 2010. Patterning a complex organ: branching morphogenesis and nephron segmentation in kidney development. *Dev Cell.* **18**, 698-712.
- Costantini F, Shakya R. 2006. GDNF/Ret signaling and the development of the kidney. *Bioessays.* **28**: 117-27.
- Davies JA. 2006. A method for cold storage and transport of viable embryonic kidney rudiments. *Kidney Int.* **70**: 2031-4.

Davies JA. 2010. The embryonic kidney: isolation, organ culture, immunostaining and RNA interference. *Method Mol Biol.* **633**: 57-69.

Favier B, Alam A, Barron P, Bonnin J, Laboudie P, Fons P, Mandron M, Herault JP, Neufeld G, Savi P, Herbert JM, Bono F. 2006. Neuropilin-2 interacts with VEGFR-2 and VEGFR-3 and promotes human endothelial cell survival and migration. *Angiogenesis.* **108**: 1243-50.

Giger RJ, Urquhart ER, Gillespie SK, Levengood DV, Ginty DD, Kolodkin AL. 1998. Neuropilin-2 Is a Receptor for Semaphorin IV: Insight into the Structural Basis of Receptor Function and Specificity. *Neuron.* **21**: 1079-92.

Guo HF, Li X, Parker MW, Waltenberger J, Becker PM, Vander Kooi CW. 2013. Mechanistic basis for the potent anti-angiogenic activity of semaphorin 3F. *Biochemistry.* **29**: 7551-8.

Guttmann-Raviv N, Shraga-Heled N, Varshavsky A, Guimaraes-Sternberg C, Kessler O, Neufeld G. 2007. Semaphorin-3A and semaphorin-3F work together to repel endothelial cells and to inhibit their survival by induction of apoptosis. *J Biol Chem.* **7**: 26294-305.

Harding SD, Armit C, Armstrong J, Brennan J, Cheng Y, Haggarty B, Houghton D, Lloyd-MacGilp S, Pi X, Roochun Y, Sharghi M, Tindal C, McMahon AP, Gottesman B, Little MH, Georgas K, Aronow BJ, Potter SS, Brunskill EW, Southard-Smith EM, Mendelsohn C, Baldock RA, Davies JA, Davidson D. 2011. The GUDMAP database - an online resource for genitourinary research. *Development.* **138**: 2845-53.

Herzog Y, Kalcheim C, Kahane N, Reshef R, Neufeld G. 2001. Differential expression of neuropilin-1 and neuropilin-2 in arteries and veins. *Mech Dev.* **109**: 115-9.

Lein ES, Hawrylycz MJ, Ao N, Ayres M, Bensinger A, Bernard A, Boe AF, Boguski MS, Brockway KS, Byrnes EJ, Chen L, Chen L, Chen TM, Chin MC, Chong J, Crook BE, Czaplinska A, Dang CN, Datta S, Dee NR, Desaki AL, Desta T, Diep E, Dolbeare TA, Donelan MJ, Dong HW, Dougherty JG, Duncan BJ, Ebbert AJ, Eichele G, Estin LK, Faber C, Facer BA, Fields R, Fischer SR, Fliss TP, Frensley C, Gates SN, Glattfelder KJ, Halverson

KR, Hart MR, Hohmann JG, Howell MP, Jeung DP, Johnson RA, Karr PT, Kawal R, Kidney JM, Knapik RH, Kuan CL, Lake JH, Laramée AR, Larsen KD, Lau C, Lemon TA, Liang AJ, Liu Y, Luong LT, Michaels J, Morgan JJ, Morgan RJ, Mortrud MT, Mosqueda NF, Ng LL, Ng R, Orta GJ, Overly CC, Pak TH, Parry SE, Pathak SD, Pearson OC, Puchalski RB, Riley ZL, Rockett HR, Rowland SA, Royall JJ, Ruiz MJ, Sarno NR, Schaffnit K, Shapovalova NV, Sivisay T, Slaughterbeck CR, Smith SC, Smith KA, Smith BI, Sodt AJ, Stewart NN, Stumpf KR, Sunkin SM, Sutram M, Tam A, Teemer CD, Thaller C, Thompson CL, Varnam LR, Visel A, Whitlock RM, Wohnoutka PE, Wolkey CK, Wong VY, Wood M, Yaylaoglu MB, Young RC, Youngstrom BL, Yuan XF, Zhang B, Zwingman TA, Jones AR. 2007. Genome-wide atlas of gene expression in the adult mouse brain. *Nature*. **445**: 168-176.

Majumdar A, Vainio S, Kispert A, McMahon J, McMahon AP. 2003. Wnt11 and Ret/Gdnf pathways cooperate in regulating ureteric branching during metanephric kidney development. *Development*. **130**: 3175-85.

Müller U, Wang D, Denda S, Meneses JJ, Pedersen RA, Reichardt LF. 1997. Integrin alpha8beta1 is critically important for epithelial-mesenchymal interactions during kidney morphogenesis. *Cell*. **88**: 603-13.

Munro DAD, Hohenstein P, Davies JA. 2017. Cycles of vascular plexus formation within the nephrogenic zone of the developing kidney. *Sci Rep*. **7**: 3273.

Nakayama H, Bruneau S, Kochupurakkal N, Coma S, Briscoe DM, Klagsbrun M. 2015. Regulation of mTOR Signaling by Semaphorin 3F-Neuropilin 2 Interactions In Vitro and In Vivo. *Sci Rep*. **5**: 11789.

Parker MW, Hellman LM, Xu P, Fried MG, Vander Kooi CW. 2010. Furin processing of semaphorin 3F determines its anti-angiogenic activity by regulating direct binding and competition for neuropilin. *Biochemistry*. **18**: 4068-75.

Procaccia V, Nakayama H, Shimizu A, Klagsbrun M. 2014. Gleevec/Imatinib, an ABL2 kinase inhibitor, protects tumor and endothelial cells from semaphorin-induced cytoskeleton collapse and loss of cell motility. *Biochem Biophys Res Commun.* **448**: 134-8.

Rao N, Lee YF, Ge R. 2015. Novel endogenous angiogenesis inhibitors and their therapeutic potential. *Acta Pharmacol Sin.* **36**: 1177-90.

Reinhoff WF. 1922. Development and growth of the metanephros or permanent kidney in chick embryos. *Johns Hopkins Hospital Bulletin.* **33**: 392-406.

Sainio K, Suvanto P, Davies J, Wartiovaara J, Wartiovaara K, Saarna M, Arumäe U, Meng X, Lindahl M, Pachnis V, Sariola H. 1997. Glial-cell-line-derived neurotrophic factor is required for bud initiation from ureteric epithelium. *Development.* **124**: 4077-87.

Sakurai A, Doçi CL, Gutkind JS. 2012. Semaphorin signaling in angiogenesis, lymphangiogenesis and cancer. *Cell Res.* **22**: 23-32.

Short KM, Combes AN, Lefevre J, Ju AL, Georgas KM, Lamberton T, Cairncross O, Rumballe BA, McMahon AP, Hamilton NA, Smyth IM, Little MH. 2014. Global quantification of tissue dynamics in the developing mouse kidney. *Dev Cell.* **29**: 188–202.

Siemerink MJ, Klaassen I, Vogels IM, Griffioen AW, Van Noorden CJ, Schlingemann RO. 2012. CD34 marks angiogenic tip cells in human vascular endothelial cell cultures. *Angiogenesis.* **15**: 151-63.

Stahl A, Joyal JS, Chen J, Sapienza P, Juan AM, Hatton CJ, Pei DT, Hurst CG, Seaward MR, Krahn NM, Dennison RJ, Greene ER, Boscolo E, Panigrahy D, Smith LE. 2012. SOCS3 is an endogenous inhibitor of pathologic angiogenesis. *Blood.* **120**: 2925-9.

Starr R, Willson TA, Viney EM, Murray LJ, Rayner JR, Jenkins BJ, Gonda TJ, Alexander WS, Metcalf D, Nicola NA, Hilton DJ. 1997. A family of cytokine-inducible inhibitors of signalling. *Nature.* **387**: 917-21.

Tanabe M, Shimizu A, Masuda Y, Kataoka M, Ishikawa A, Wakamatsu K, Mii A, Fujita E, Higo S, Kaneko T, Kawachi H, Fukuda Y. 2012. Development of lymphatic vasculature and morphological characterization in rat kidney. *Clin Exp Nephrol.* **16**: 833-42.

Villegas G, Tufro A. 2002. Ontogeny of semaphorins 3A and 3F and their receptors neuropilins 1 and 2 in the kidney. *Mech Dev.* **119**: S149-53.

Walz A, Feinstein P, Khan M, Mombaerts P. 2007. Axonal wiring of guanylate cyclase-D-expressing olfactory neurons is dependent on neuropilin 2 and semaphorin 3F. *Development.* **134**: 4063-72.

Xiang W, Ke Z, Zhang Y, Cheng GH, Irwan ID, Sulochana KN, Potturi P, Wang Z, Yang H, Wang J, Zhuo L, Kini RM, Ge R. 2011. Isthmin is a novel secreted angiogenesis inhibitor that inhibits tumour growth in mice. *J Cell Mol Med.* **15**: 359-74.

Zhang Y, Chen M, Venugopal S, Zhou Y, Xiang W, Li YH, Lin Q, Kini RM, Chong YS, Ge R. 2011. Isthmin exerts pro-survival and death-promoting effect on endothelial cells through $\alpha 5 \beta 1$ integrin depending on its physical state. *Cell Death Dis.* **2**: e153.

Figure legends

Figure 1. Selection of *Sema3f* as a candidate gene for vascular plexus patterning in kidney development. (A) Cartoons portraying the relevant cell populations in the nephrogenic zone of the kidney (modified GUDMAP cartoons). Note that the vasculature forms within the nephrogenic interstitium and around the cap mesenchyme. (B) Criteria for candidate gene selection. (C) GUDMAP microarray heatmap data showing the expression of the top three anti-angiogenic candidate genes by the cap mesenchyme at E15.5 and P0-P4: reproduced under the terms of the GUDMAP licence for re-use. (D) Expression of the top three candidate genes in the nephrogenic interstitium at E15.5 (relative to the cap mesenchyme). (E) Expression of the receptors for *Ism1* (*Grp78* and *Itgav*) and *Sema3f* (*Nrp1* and *Nrp2*) by various renal endothelial beds at E15.5.

Figure 2. Microarray heatmap data from GUDMAP showing the relative expression of anti-angiogenic genes by the cap mesenchyme at E15.5 and P0-P4. This list of anti-angiogenic genes is not exhaustive. Heatmap data is reproduced under the terms of the GUDMAP licence for re-use.

Figure 3. Confirmation that *Sema3f* is expressed in the cap mesenchyme of the developing kidney. (A-A') In situ hybridisation image showing *Sema3f* expression in the cap mesenchyme of the E15.5 kidney (from GUDMAP; submitted by the McMahon lab). (B-C') In situ hybridisation images showing *Sema3f* expression in the (B-B') E11.5 and (C-C') E13.5 kidney (image credit: Allen Institute). (D) E12.5 kidney co-stained with anti-*Sema3f* and anti-*Gata3*. Red blood cells are yellow (due to heme auto-fluorescence in the red and green channels as a result of tissue clearing). (E) E15.5 kidney co-stained with anti-*Sema3f* and anti-integrin alpha-8 (*ITGA8*). Negative control (secondary only) image was taken using

identical microscope settings. Scale bars = 100 μm (except from **B-C'** where scale bar values are stated).

Figure 4. Expression of Nrp2 by endothelial cells in the nephrogenic interstitium. (A) Nrp2⁺ cells within the nephrogenic interstitium are endothelial. **(B)** As the cap mesenchyme splits, Nrp2⁺ endothelia are present at the bifurcation site where new vascular plexuses form (white arrowhead shows an example). **(C)** Nrp2⁺ endothelia are positioned around the cap mesenchyme. **(D)** Cartoon illustrating the complementary expression pattern of Nrp2 and Sema3f in the nephrogenic zone. Green arrowheads indicate the direction of endothelial migration as cap mesenchymal populations split. Scale bars = 100 μm .

Figure 5. Expression of Nrp1 and Nrp2 in the endothelia of the ureter. (A) Based on vessel morphology in the E18.5 ureter, veins (V; larger diameter vessel with loosely packed endothelia) are CD31⁺Nrp2⁺, whereas arteries (A; smaller diameter vessel with tightly packed endothelia) are CD31⁺Nrp2⁻. **(B-C')** Based on co-staining in the E18.5 ureter, **(B)** lymphatic vessels are Nrp2⁺Lyve-1⁺CD31⁺, **(C-C')** veins are Nrp2⁺EphB4⁺Nrp1⁻, and arteries are Nrp1⁺Nrp2⁻EphB4⁻. Macrophages (M Φ) are also present in **B**. A, artery; V, vein; LV, lymphatic vessel; M Φ , macrophages. Scale bars = 100 μm .

Figure 6. Nrp1 and Nrp2 expression in the developing kidney. (A-C) Expression of Nrp1 and Nrp2 by renal endothelia at E11.5-E13.5. **(D)** Cartoons illustrating the expression patterns of Nrp1 and Nrp2 and the position of the cap mesenchyme (CM) in the E11.5-E13.5 kidney. **(E-F)** Nrp1 and Nrp2 expression in plexus endothelia at **(E)** E13.5 and **(F)** E18.5. Scale bars = 100 μm .

Figure 7. Nrp2 expression in lymphatic endothelia. (A) A network of Nrp2⁺ lymphatic vessels surround the major arteries in the kidney, mesonephros, gonad, and adrenal gland (stitched confocal z-stacks; 2x2 tiles; 57 images per tile). **(B)** Renal Nrp2⁺ lymphatic vessels

connect with the $Nrp2^+$ lymphatic vessels in the ureter (representative image of $n = 4$ confocal z-stack images). **(C)** Lymphatic vessels form alongside the segmental vasculature. Red blood cells are magenta (due to heme auto-fluorescence in the red and blue channels as a result of tissue clearing). AG, adrenal gland. Scale bars = 100 μm .

Figure 8. Sema3f and Nrp2 are not required for exclusion of blood vessels from the cap mesenchyme in the nephrogenic zone. (A-B) Genetic ablation of *Sema3f* had no effect on vascular patterning around the caps (representative images from $n = 2-3$ P0 mice; 4-6 kidneys per genotype; 9-12 total fields of staining per genotype). **(C-D)** Genetic ablation of *Nrp2* had no effect on vascular patterning around the caps (representative images from $n = 1-3$ E18.5 embryos; 2-6 total fields of staining per genotype). Asterisks in the genotyping gel images represent the embryos/pups whose kidneys are shown in the representative images. Scale bars = 100 μm .

Supplementary figure legend

Supplementary Movie 1. Confocal z-stack images of an E15.5 *Nrp2*-EGFP kidney. White arrows show examples of $Nrp2^+$ cells in the nephrogenic interstitium. White arrowheads show examples of $Nrp2^+$ proximal tubules. Video adapted from data generated by the Potter lab.

Supplementary Movie 2. Tiled z-stack images of the $Nrp2^+$ network of lymphatic vessels in the E15.5 kidney and adjacent organs. Vessels were rendered using the volume tool in IMARIS.

Figures

Figure 1. Prepared for two columns.

Figure 2. Prepared for two columns.

Figure 3. Prepared for two columns.

Figure 4. Prepared for two columns.

Figure 5. Prepared for one column.

Figure 6. Prepared for two columns.

Figure 7. Prepared for two columns.

Figure 8: Prepared for two columns.

Accepted Article

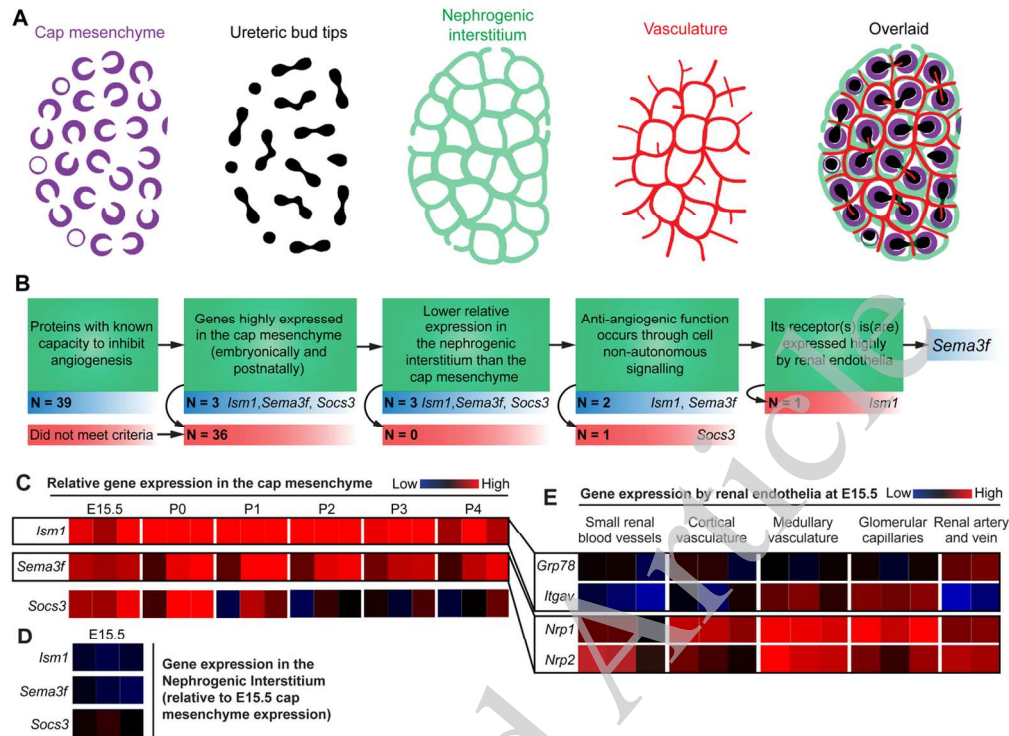


Figure 1. Selection of *Sema3f* as a candidate gene for vascular plexus patterning in kidney development. (A) Cartoons portraying the relevant cell populations in the nephrogenic zone of the kidney (modified GUDMAP cartoons). Note that the vasculature forms within the nephrogenic interstitium and around the cap mesenchyme. (B) Criteria for candidate gene selection. (C) GUDMAP microarray heatmap data showing the expression of the top three anti-angiogenic candidate genes by the cap mesenchyme at E15.5 and P0-P4; reproduced under the terms of the GUDMAP licence for re-use. (D) Expression of the top three candidate genes in the nephrogenic interstitium at E15.5 (relative to the cap mesenchyme). (E) Expression of the receptors for *Ism1* (*Grp78* and *Itgav*) and *Sema3f* (*Nrp1* and *Nrp2*) by various renal endothelial beds at E15.5.

129x95mm (300 x 300 DPI)

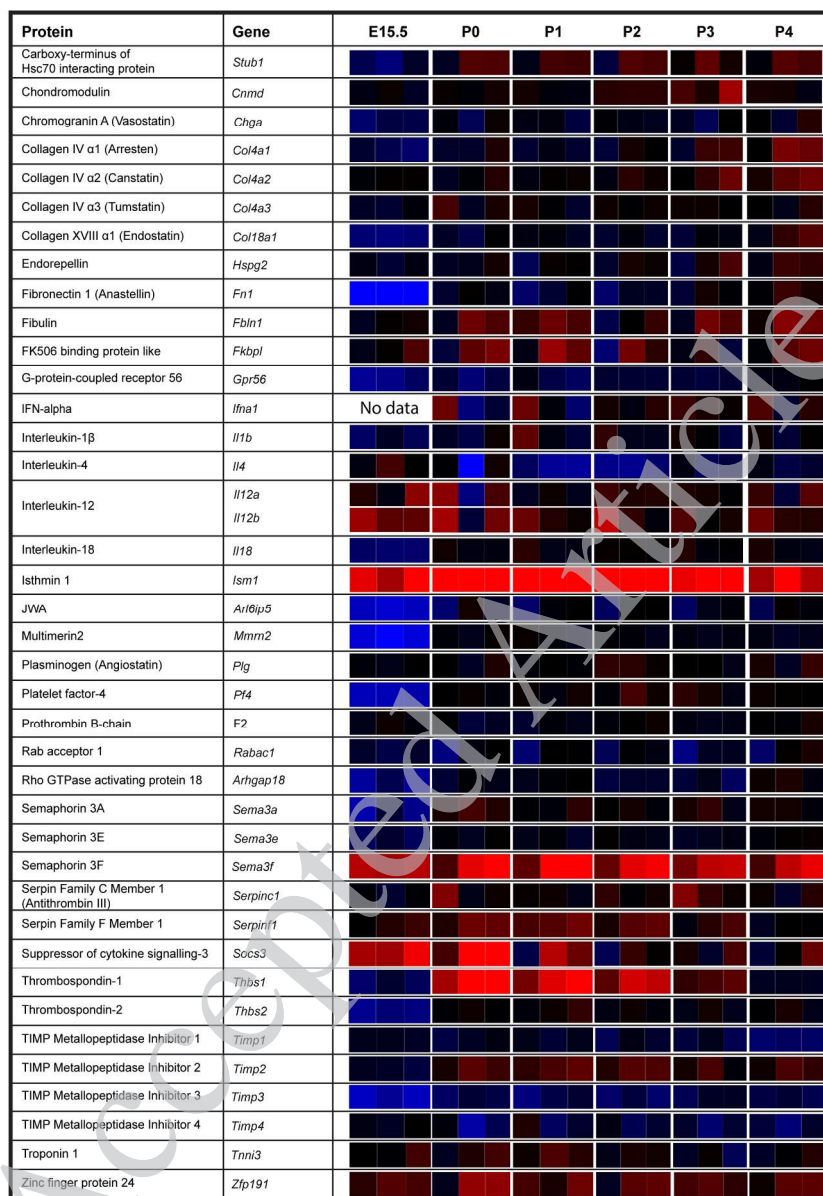


Figure 2. Microarray heatmap data from GUDMAP showing the relative expression of anti-angiogenic genes by the cap mesenchyme at E15.5 and P0-P4. This list of anti-angiogenic genes is not exhaustive. Heatmap data is reproduced under the terms of the GUDMAP licence for re-use.

159x227mm (300 x 300 DPI)

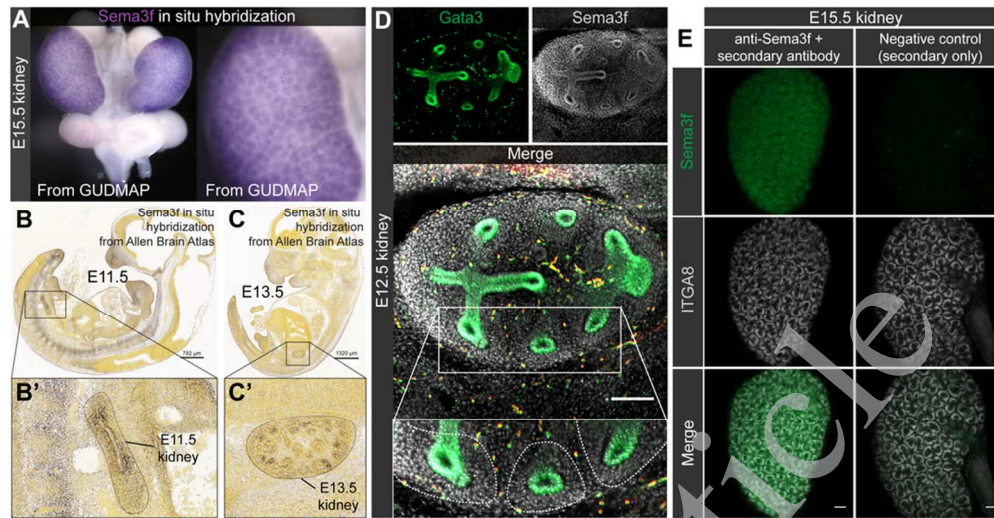


Figure 3. Confirmation that *Sema3f* is expressed in the cap mesenchyme of the developing kidney. (A-A') In situ hybridisation image showing *Sema3f* expression in the cap mesenchyme of the E15.5 kidney (from GUDMAP; submitted by the McMahon lab). (B-C') In situ hybridisation images showing *Sema3f* expression in the (B-B') E11.5 and (C-C') E13.5 kidney (image credit: Allen Institute). (D) E12.5 kidney co-stained with anti-*Sema3f* and anti-Gata3. Red blood cells are yellow (due to heme auto-fluorescence in the red and green channels as a result of tissue clearing). (E) E15.5 kidney co-stained with anti-*Sema3f* and anti-integrin alpha-8 (ITGA8). Negative control (secondary only) image was taken using identical microscope settings. Scale bars = 100 μm (except from B-C' where scale bar values are stated).

91x47mm (300 x 300 DPI)

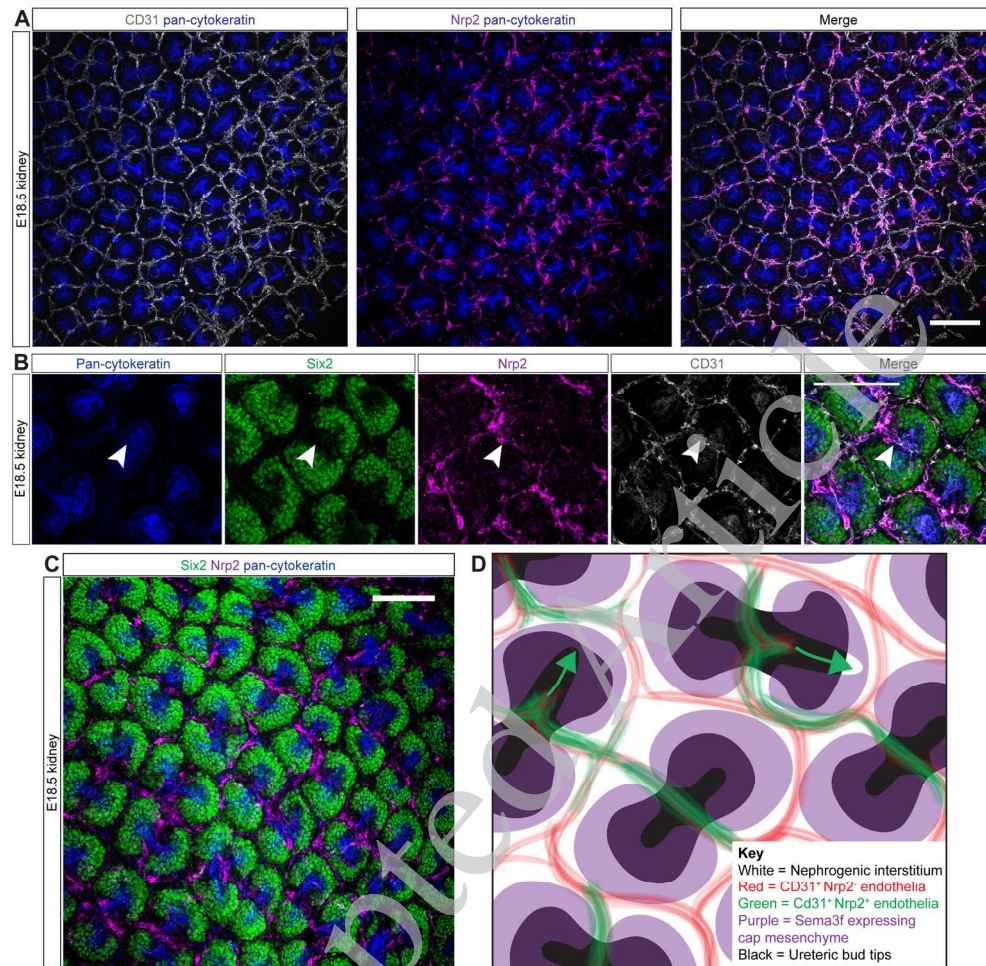


Figure 4. Expression of Nrp2 by endothelial cells in the nephrogenic interstitium. (A) Nrp2+ cells within the nephrogenic interstitium are endothelial. (B) As the cap mesenchyme splits, Nrp2+ endothelia are present at the bifurcation site where new vascular plexuses form (white arrowhead shows an example). (C) Nrp2+ endothelia are positioned around the cap mesenchyme. (D) Cartoon illustrating the complementary expression pattern of Nrp2 and Sema3f in the nephrogenic zone. Green arrowheads indicate the direction of endothelial migration as cap mesenchymal populations split. Scale bars = 100 μ m.

170x165mm (300 x 300 DPI)

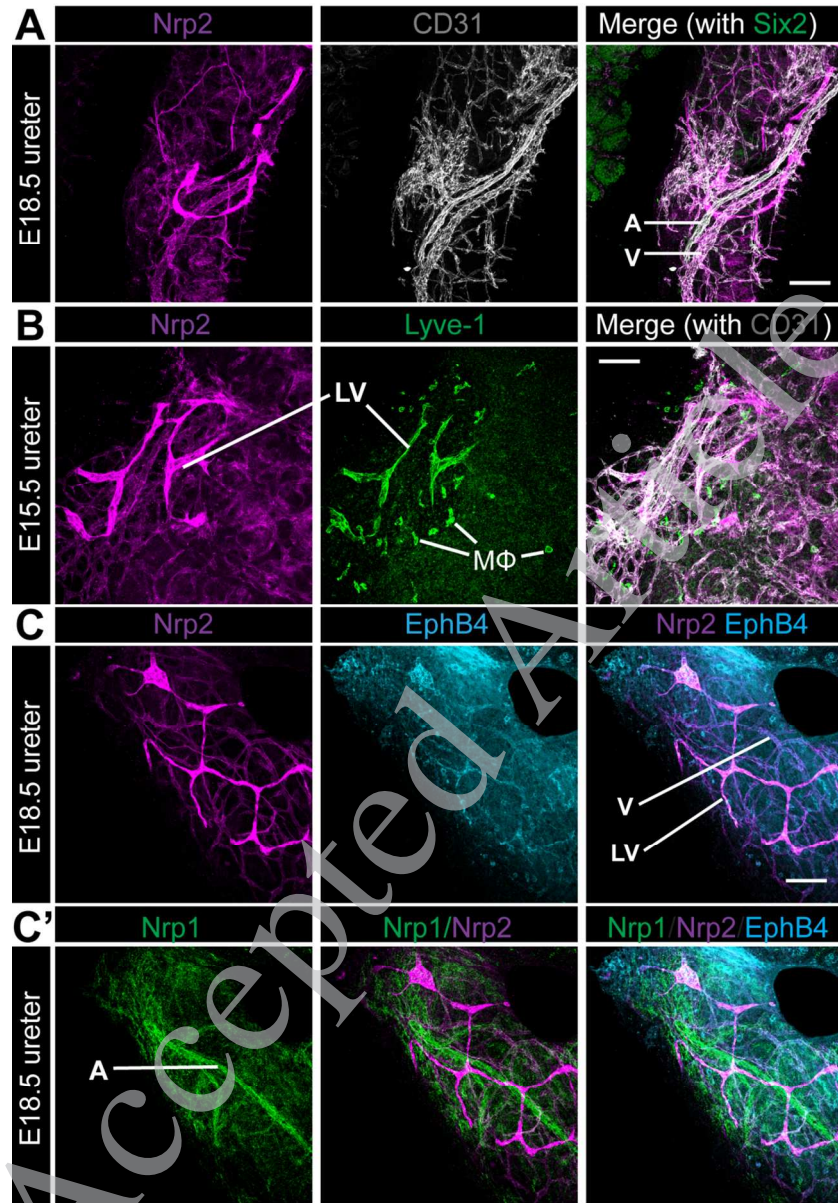


Figure 5. Expression of Nrp1 and Nrp2 in the endothelia of the ureter. (A) Based on vessel morphology in the E18.5 ureter, veins (V; larger diameter vessel with loosely packed endothelia) are CD31+Nrp2+ whereas arteries (A; smaller diameter vessel with tightly packed endothelia) are CD31+Nrp2-. (B-C') Based on co-staining in the E18.5 ureter, (B) lymphatic vessels are Nrp2+Lyve-1+CD31+, (C-C') veins are Nrp2+EphB4+Nrp1- and arteries are Nrp1+Nrp2-EphB4-. Macrophages (MΦ) are also present in B. A, artery; V, vein; LV, lymphatic vessel; MΦ, macrophages. Scale bars = 100 μ m.

120x173mm (300 x 300 DPI)

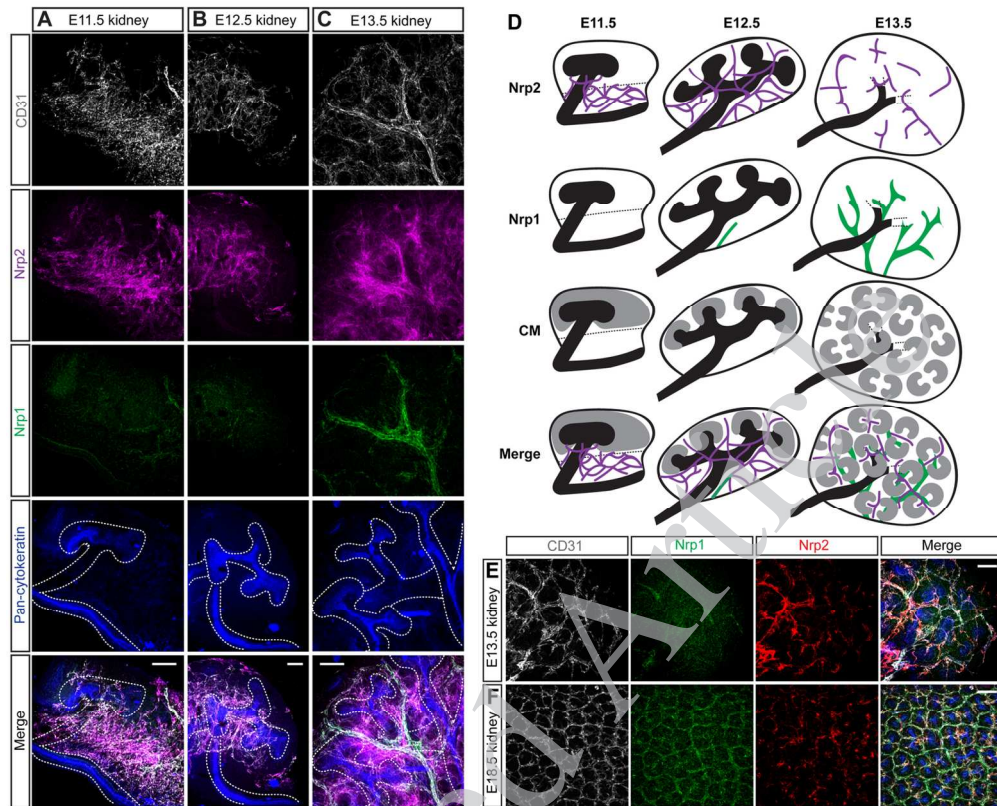


Figure 6. Nrp1 and Nrp2 expression in the developing kidney. (A-C) Expression of Nrp1 and Nrp2 by renal endothelia at E11.5-E13.5. (D) Cartoons illustrating the expression patterns of Nrp1 and Nrp2 and the position of the cap mesenchyme (CM) in the E11.5-E13.5 kidney. (E-F) Nrp1 and Nrp2 expression in plexus endothelia at (E) E13.5 and (F) E18.5. Scale bars = 100 μ m.

141x114mm (300 x 300 DPI)

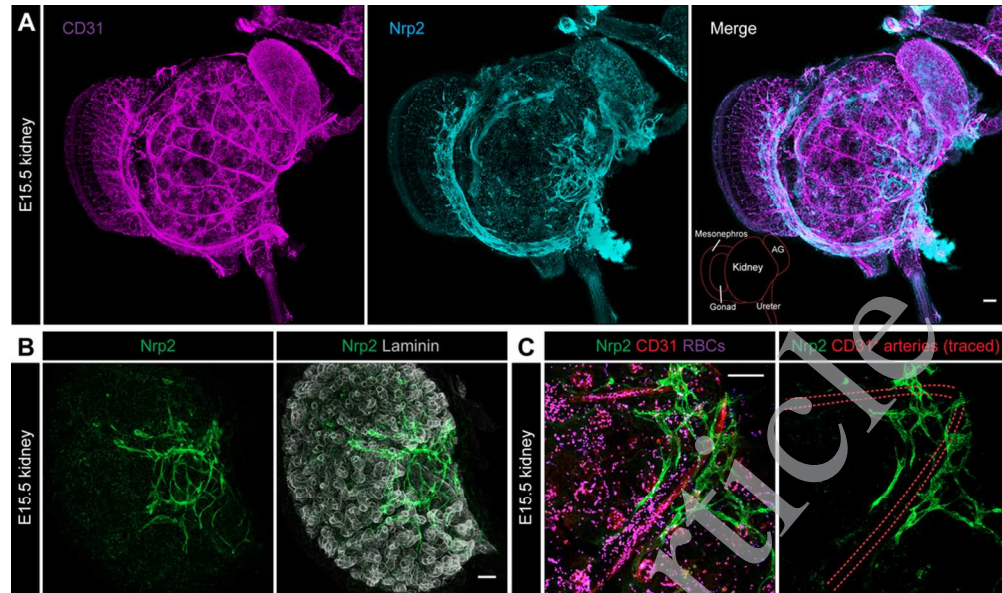


Figure 7. Nrp2 expression in lymphatic endothelia. (A) A network of Nrp2+ lymphatic vessels surround the major arteries in the kidney, mesonephros, gonad, and adrenal gland (stitched confocal z-stacks; 2x2 tiles; 57 images per tile). (B) Renal Nrp2+ lymphatic vessels connect with the Nrp2+ lymphatic vessels in the ureter (representative image of $n = 4$ confocal z-stack images). (C) Lymphatic vessels form alongside the segmental vasculature. Red blood cells are magenta (due to heme auto-fluorescence in the red and blue channels as a result of tissue clearing). AG, adrenal gland. Scale bars = 100 μm .

101x59mm (300 x 300 DPI)

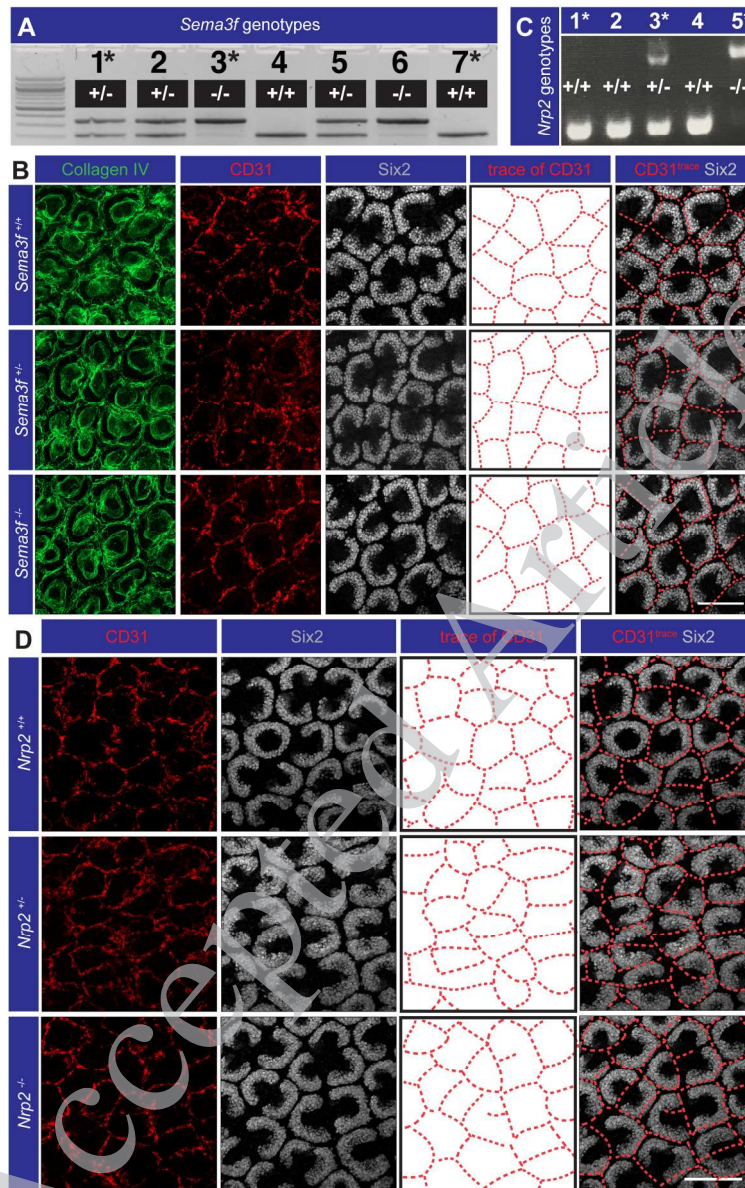


Figure 8. *Sema3f* and *Nrp2* are not required for exclusion of blood vessels from the cap mesenchyme in the nephrogenic zone. (A-B) Genetic ablation of *Sema3f* had no effect on vascular patterning around the caps (representative images from $n = 2-3$ P0 mice; 4-6 kidneys per genotype; 9-12 total fields of staining per genotype). (C-D) Genetic ablation of *Nrp2* had no effect on vascular patterning around the caps (representative images from $n = 1-3$ E18.5 embryos; 2-6 total fields of staining per genotype). Asterisks in the genotyping gel images represent the embryos/pups whose kidneys are shown in the representative images. Scale bars = 100 μm .

200x322mm (300 x 300 DPI)